JACS
JOURNAL OF THE AMERICAN CHEMICAL SOCIETY

ARTICLE

pubs.acs.org/JACS

Peptide Conformational Preferences in Osmolyte Solutions: Transfer Free Energies of Decaalanine

Hironori Kokubo,[†] Char Y. Hu,[†,‡] and B. Montgomery Pettitt*[,†,‡]

[†]Department of Chemistry, University of Houston, Houston, Texas 77204-5003, United States

[‡]Graduate Program in Structural and Computational Biology and Molecular Biophysics, Baylor College of Medicine, Houston, Texas 77030, United States

ABSTRACT: The nature in which the protecting osmolyte trimethylamine *N*-oxide (TMAO) and the denaturing osmolyte urea affect protein stability is investigated, simulating a decaalanine peptide model in multiple conformations of the denatured ensemble. Binary solutions of both osmolytes and mixed osmolyte solutions at physiologically relevant concentrations of 2:1 (urea:TMAO) are studied using standard molecular dynamics simulations and solvation free energy calculations. Component analysis reveals the differences in the importance of the van der Waals (vdW) and electrostatic interactions for protecting and denaturing osmolytes. We find that urea denaturation governed by transfer free energy differences is dominated by vdW attractions, whereas TMAO exerts its effect by causing unfavorable electrostatic interactions both in the binary solution and mixed osmolyte solution. Analysis of the results showed no evidence in the ternary solution of disruption of the correlations among the peptide and osmolytes, nor of significant changes in the strength of the water hydrogen bond network.

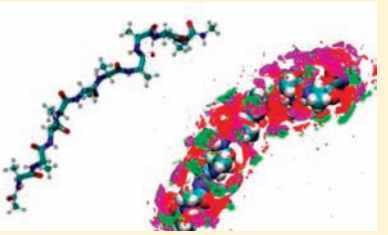

1. INTRODUCTION

In response to a variety of environmental stresses, numerous organisms have selectively adapted the usage of organic osmolytes to maintain cellular integrity. Regulation of these small organic compounds helps to maintain cellular water levels and thus cellular volume.[1−3] An additional benefit of many organic osmolytes is the ability to stabilize proteins.[4] While the study of the effect of an individual osmolyte on a protein has received much attention, there has been far less examination of solutions consisting of multiple osmolyte species. Many organisms have adapted such systems whereby the tandem usage of osmolytes serves to balance differing protein stabilizing effects. For instance, to counteract the accumulation of the denaturing osmolyte urea, cartilaginous fishes accumulate the protecting osmolyte trimethylamine *N*-oxide (TMAO) at physiological concentrations of urea to TMAO concentration of 2:1.[5,6] Furthermore, it has been suggested that TMAO counteraction of urea denaturation is independent of whether the protein evolved in such a solvent environment and is thus a universal property of the osmolyte solution.[7]

The osmolyte effect on protein stability has been explained by thermodynamic interactions or correlations between the osmolyte and the protein backbone. Protecting osmolytes (such as sarcosine, trimethylamine *N*-oxide, sucrose, and proline to name a few) have unfavorable interactions with the protein backbone and thus increase the stability of proteins.[8,9] This is in contrast with urea, where it is the favorable interactions of the denaturing osmolyte and the protein backbone that destabilizes the protein.[8−11]

An intuitive mechanism for osmolyte counteraction would be if the addition of the protecting osmolyte species to the urea solution serves to disrupt the favorable interactions and correlations between urea and the protein backbone. However, by studying the experimental unfolding transition of two proteins, it was shown that urea unfolding was independent of the presence of TMAO.[12] Similarly, direct calculation of thermodynamic *m*-values (related to the change in free energy with respect to osmolyte concentration) of mixture solutions of protecting osmolytes TMAO and sarcosine coupled with urea demonstrated no effect on the individual *m*-values of either osmolyte component.[13] This lack of interference by either osmolyte species could be due to the low site occupancy of the osmolytes.[13] Simulations of TMAO and urea solution mixtures have shown a lack of disruption of the neopentane interactions, making it unlikely that TMAO counteraction occurs by interfering with the hydrophobic effect.[14,15] This is confirmed by experiments on the transfer free energy difference between water and TMAO solution for hydrophobic side-chain model compounds.[16]

Thus, the mechanism by which competing osmolytes interact in solution to produce a counterbalanced effect has yet to be completely defined. Here, we model urea−TMAO solution mixtures, as well as binary osmolyte solutions, in order to study the solvation characteristics of mixed osmolyte solutions. Solvation free energy calculations were carried out for a decaalanine peptide in five different conformations ranging from extended to helix. The solvation free energy and transfer free energy of each peptide conformation were calculated in four solutions: pure water, TMAO, urea, and mixed TMAO/urea solution. Component analysis of the free energy values provides insight into the

Received: September 9, 2010
Published: January 20, 2011

dx.doi.org/10.1021/ja1078128 | *J. Am. Chem. Soc.* 2011, 133, 1849–1858

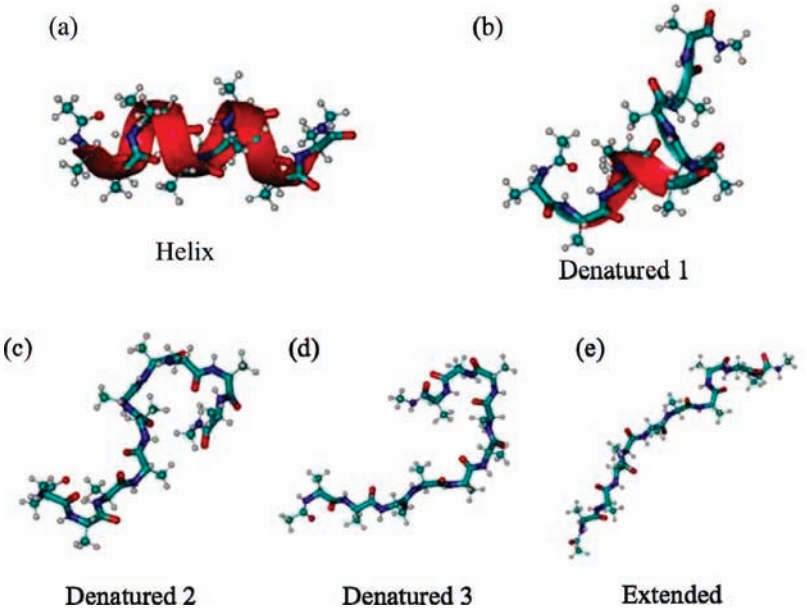

Figure 1. Five fixed peptide conformations.

mechanism of TMAO counteraction of urea denaturation. Furthermore, comparisons with standard molecular dynamics simulations of the peptide conformations in each solution were carried out in order to identify at a molecular level whether either osmolyte affects the interactions of the additional osmolyte species.

2. METHODS

2.1. MD Simulations. The all atom parameter set Amber ff03[17] was used for the alanine peptide, while the force field parameters for the TMAO and urea molecules were adopted from Kast et al[18] and Smith,[19] respectively. The Kirkwood−Buff Force Field (KBFF) urea model of Smith and co-workers takes the challenging approach of fitting the charge distribution to the experimental activity coefficient data.[19] For the solvent, consistent with the Amber force field, we chose the TIP3P model for water in our simulations.[20] The force field used determines the quantitative outcome in simulation studies such as these. We prepared models of an alanine decapeptide in water, 4 M TMAO solution, 8 M urea solution, and a 4 M TMAO/8 M urea solution mixture as described previously.[21,22]

To prepare our solutions, we took an equilibrated TMAO box, urea box, and water box and randomly removed the number of TMAO, urea, and water molecules from each of the boxes to achieve the required solvent amounts for the desired solution concentrations. Subsequently, the three boxes were placed in contact expanding the normal periodic boundary conditions to the volume equivalent to the two (or three) pure liquids. We then performed an energy minimization of 500 steps and allowed mixing to occur using 100 ps of NVT simulation for each concentration. The temperature was held to 298 K by the Nosé method.[23] We next performed 300 ps long NPT simulations for further equilibration at 298 K and 1 atm, using the Nosé−Anderson method for controlling the temperature and pressure.[23,24] In this process it was found that the mixing occurred not only spontaneously, but in fact quite rapidly, on the order of the time it took to shrink the box to achieve the target temperature and pressure, 298 K and 1 atm. We immersed an alanine peptide with a helix conformation into these four solutions by removing the overlapping solvent molecules. We again performed an energy minimization for 500 steps and NVT simulation for 100 ps for each concentration. Following this, 1.0 ns long NPT equilibration simulations were carried out using an integration time step of 1.0 fs and the RATTLE method to fix the bond lengths.[25] The final system sizes were close to 41 Å × 41 Å × 41 Å in each case, allowing us to use the same cutoff length of 15 Å for the vdW interactions. We used a fast linked-cell Ewald method for electrostatic interactions with the r-space cutoff and Ewald convergence parameter α set to 1.5 and 2.09 nm^{-1}, respectively.[26]

We performed 10 ns replica exchange simulations (REM) for all four solution systems (details below) and chose five representative peptide conformations, designated as helix, denatured 1, denatured 2, denatured 3, and extended (see Figure 1). The nonhelical conformations were chosen at random from conformational clusters in a free simulation that were not associated with the initial helix. We then calculated the solvation free energy of these five conformations. The number of total systems prepared is thus 20, that is, five fixed peptide conformations in four different solutions. We list all the simulation systems in Table 1. We calculated the solvation free energy of these five fixed peptide conformations in four different solutions by adopting the replica-exchange λ sampling method outlined below.

2.2. Replica-Exchange λ Sampling. Replica exchange is a powerful simulation method to enhance and help ensure good sampling. Here, as in previous works,[27,28] we use the technique to aid in the free energy sampling problem. Briefly, the λ parameter is the so-called charging or coupling variable in free energy thermodynamic integrations.[29] In the original replica-exchange method, temperatures of a pair of neighboring replicas are exchanged during the simulation, whereas in this method the λ parameters are exchanged instead. This can be considered to be a variation on the theme of Hamiltonian replica-exchange methods such as those proposed by Takada[30] and Sugita.[31]

The generalized ensemble for replica-exchange λ sampling consists of M noninteracting replicas of the original system in the canonical ensemble at M different λ parameters, that is, λ_m (m = 1, 2, ..., M). One replica has one λ parameter such that replica i and λ_m are in one-to-one correspondence. The Hamiltonian for the ith replica at λ_m is

$$H_m(q^{[i]}, p^{[i]}) = K(p^{[i]}) + E_{\lambda_m}(q^{[i]}) \quad (1)$$

where $q^{[i]}$ and $p^{[i]}$ are coordinate vectors and momentum vectors of replica i, respectively. $K(p^{[i]})$ is the kinetic energy, and $E_{\lambda m}$ $(q^{[i]})$ is the potential energy for $\lambda = \lambda_m$. $E_{\lambda m}$ $(q^{[i]})$ has potential energy terms that differ from the original only between the molecule for which we calculate the solvation free energy and all other molecules. As the replicas are

Table 1. Twenty Nanosecond NPT Simulation Systems with the Five Fixed Peptide Conformations in Four Different Solutions[a]

	N_{ala}	N_t	N_u	N_w	N_{atom}	volume	density
a1a10w	1	0	0	2210	6712	69.45−69.60	0.969−0.967
a1a10tw	1	156	0	1604	7108	71.00−71.22	0.965−0.968
a1a10uw	1	0	308	1376	6704	67.45−67.60	1.083−1.085
a1a10tuw	1	154	308	837	7243	70.67−70.87	1.076−1.079

[a] ala10w, ala10tw, ala10uw, and ala10tuw are decaalanine in water, in 4 M TMAO solution, in 8 M urea solution, and in 4 M TMAO/8 M urea solution, respectively. Symbols are N_{ala}: number of alanine peptide, N_t: number of TMAO molecules, N_u: number of urea molecules, N_w: number of water molecules. The volume and the density show the range of average for the simulations with fixed peptide conformations. The units of volume and density are (nm^3) and (g/cm^3), respectively.

noninteracting, the weight factor is simply the product of the Boltzmann factors for each replica.

$$W = \exp\left\{ -\sum_{i=w}^{M} \beta H_{m(i)}(q^{[i]}, q^{[i]}) \right\} \quad (2)$$

Here, $m(i)$ is the λ parameter of replica i. The simulation is then performed according to the following procedures. First, a simulation in the canonical ensemble using a fixed value of the λ parameter is carried out independently. Next, a pair of replicas are exchanged with the probability $w(x_m^{[i]}x_n^{[j]})$, with $x_m^{[i]}$ and $x_n^{[j]}$ defined to mean that replica i has $\lambda = \lambda_m$ and replica j has $\lambda = \lambda_n$. The exchange probability between these two replicas, $w(x_m^{[i]}x_n^{[j]})$, is

$$w(x_m^{[i]}x_n^{[j]}) = \begin{cases} 1, & \text{for } \Delta \le 0 \\ \exp(-\Delta), & \text{for } \Delta > 0 \end{cases} \quad (3)$$

where

$$\Delta = \beta(E_{\lambda_m}(q^{[j]}) - E_{\lambda_m}(q^{[i]}) - E_{\lambda_n}(q^{[j]}) + E_{\lambda_n}(q^{[i]})) \quad (4)$$

These two steps are repeated at intervals during a simulation.

We used the following soft core potential for the vdW term calculations to avoid the well-known numerical singularity while calculating the free energy difference.[32,33]

$$U(\lambda_m) = \lambda_m \left\{ 4\varepsilon_{ij} \left[\frac{1}{\left(\alpha_{ij}(1-\lambda_m)^2 + \left(\frac{r_{ij}}{\sigma_{ij}}\right)^6\right)^2} - \frac{1}{\left(\alpha_{ij}(1-\lambda_m)^2 + \left(\frac{r_{ij}}{\sigma_{ij}}\right)^6\right)} \right] \right\} \quad (5)$$

We first calculated the vdW component of the solvation free energy and then calculated the electrostatic component using the full extent of the vdW potential. Because there is no singularity after completing the vdW sphere, we can safely use simple linear scaling for the electrostatic component. We used the following 28 intermediate λ points for the calculation of the vdW component: 0.000, 0.100, 0.150, 0.200, 0.230, 0.255, 0.270, 0.285, 0.300, 0.310, 0.320, 0.330, 0.345, 0.360, 0.380, 0.400, 0.425, 0.455, 0.485, 0.520, 0.560, 0.600, 0.650, 0.700, 0.750, 0.800, 0.900, and 1.000. More points are needed near the peak in the vdW λ sampling, whereas the electrostatics profile is quite smooth with respect to λ and so only 11 intermediate λ points were used: 0.0, 0.1, 0.2, 0.3, 0.4, 0.5, 0.6, 0.7, 0.8, 0.9, and 1.0. To guarantee sufficient sampling, the number of λ points and their distribution were selected from the preliminary short runs in order to obtain a sufficient acceptance ratio between the neighboring points, with λ exchange being attempted every picosecond.

The results of the calculations were divided into vdW and electrostatic components as follows: the vdW contribution were calculated first, followed by the electrostatic component with the full (normal) vdW interactions already on. While these components of free energy can be path dependent our procedure is well-defined and we will consider the value of the results of this decomposition in context. We then performed 20 independent solvation free energy calculations of five fixed peptide conformations in four different solutions: pure water, 4 M TMAO, 8 M urea, and 4 M TMAO/8 M urea solution.

We verified that every replica experiences a random walk in replica space for both the electrostatic and vdW components (data not shown). With each simulation, via replica-exchange λ sampling we are able to obtain the solvation free energy using three different, well-known methods simultaneously: thermodynamic integration, the perturbation method, and Bennett acceptance ratio method. With the thermodynamic integration method, the solvation free energy is estimated by numerically integrating these points. Alternatively, the solvation free energy can be calculated by the perturbation method or Bennett acceptance method (similar to the weighted histogram technique). We confirmed that all three calculation methods produced very similar results (data not shown). We also confirmed that the perturbation method produced the worse estimation when the available time series data was decreased (data not shown). It is known that the Bennett acceptance method is a better estimator than the perturbation method;[34,35] therefore, we report values from the Bennett acceptance method below.

The advantage of the replica-exchange sampling method is that we can determine a sufficient (and efficient) number of intermediate λ points and distributions by checking the exchange acceptance ratios of the neighboring λ's from a few short preliminary runs. Sufficient sampling overlap between the neighboring replicas guarantees good sampling for the replica exchanges. In addition, we found that different configurational sampling from different replicas is obtained through λ exchange, which improves the sampling efficiency especially when a strong electrostatic or vdW interaction between specific molecules would cause sampling problems (remain for a long time) for regular MD simulation. Such interactions are changed and the reorganization of the surroundings thus enhanced through λ exchange. Replica-exchange λ sampling can be performed at comparable time scales to standard simulations, because the time consumed by the λ exchange is negligible.

3. RESULTS AND DISCUSSION

Classically, the effects of varying solvent composition are decomposed into electrostatic and hydrophobic effects. Recent reexamination of the classic Tanford experiments on contributions to change in solvation free energy differences,[16] along with consideration of what constitutes hydrophobicity,[36] brings into question this taxonomy. Here we prefer to use a more natural set of variables, electrostatic and van der Waals interactions, which are conveniently part of the underlying intermolecular interaction models, to show the mechanistic trends of solution (de) stabilization.

We performed replica-exchange λ sampling simulations to calculate the solvation free energy of the selected conformations of a decaalanine peptide in osmolyte solution. Figure 1 shows the five peptide conformations ranging from helix to extended. Table 2 shows selected properties of these five conformations.

The total solvation free energy and the vdW and electrostatic components of the solvation free energy of the peptide conformations in each solution are shown in Figure 2. For each conformation, the total solvation free energy is bounded by the most favorable in urea solution and the least favorable in TMAO solution, as expected. Additionally, the compensatory effect of

Table 2. Basic Properties of Five Fixed Peptide Conformations[a]

	rmsd	RG	SA	END
helix	0.32	5.8	1068	17.3
denatured 1	3.0	6.0	1130	14.4
denatured 2	3.8	7.0	1220	14.8
denatured 3	4.5	8.0	1350	15.6
extended	7.1	10.2	1453	33.3

[a] The abbreviations are RMSD [Å]: root-mean-square deviation of heavy atoms from ideal helix conformation, RG [Å]: radius of gyration, SA [Å^2]: solvent-accessible surface area proved by 1.6 Å sphere, END [Å]: end-to-end distance.

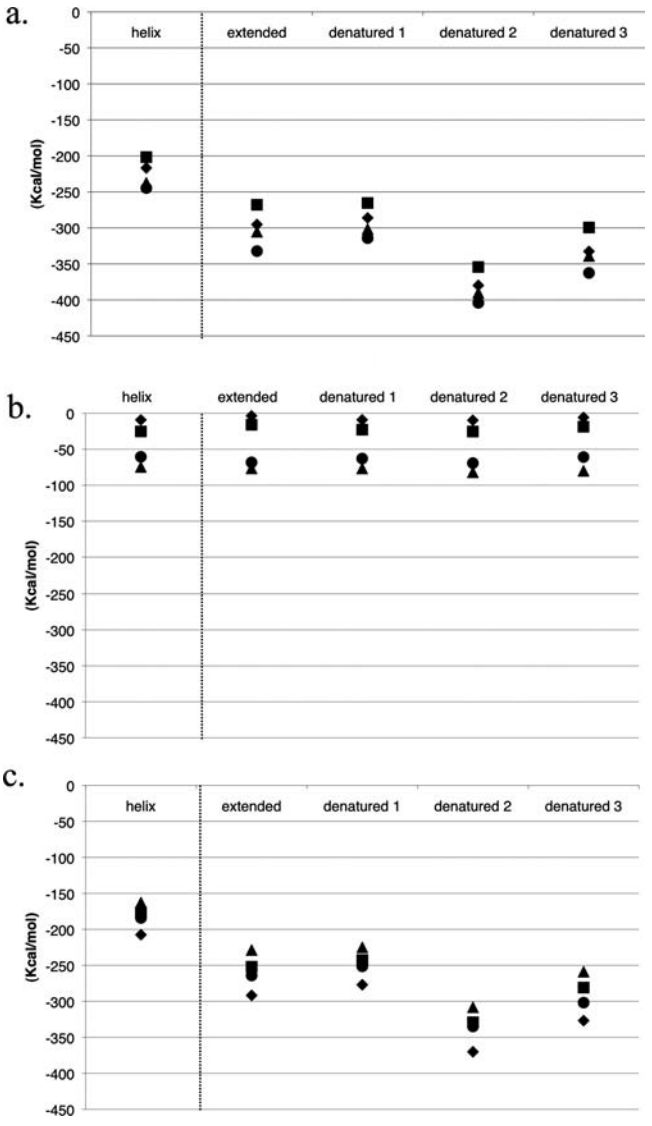

Figure 2. Solvation free energy. (a) Total solvation free energy, (b) vdW component, and (c) electrostatic component of the solvation free energy. Diamonds: water, squares: 4 M TMAO solution, circles: 8 M urea solution, triangles: 4 M TMAO/8 M urea solution.

TMAO is seen in Figure 2a, in that the solvation free energy of each conformation in the osmolyte mixture solution approaches that of the values in pure water solution. Analyzing the component contributions to the solvation free energy potentially allows for insight into the thermodynamics of the osmolyte effect on protein stability.

From the data in Figure 2b, based on the vdW component, water has the least favorable contribution (highest component free energy value) with the ternary solution having the most favorable (lowest energy value). It is interesting that the compensatory effect of TMAO is not evident in the vdW component profile; rather TMAO enhances the favorable vdW solvation free energy of the peptide compared to pure water. Both urea and TMAO have more favorable vdW effects on the peptide than water. We also see that the urea vdW component is more favorable than TMAO. Considering that the vdW term represents short-range interactions, this tendency suggests that urea is making better vdW contacts with the peptides than TMAO, perhaps due to the planar shape of urea allowing better geometry for vdW interactions with the peptide than TMAO and water. Additionally, we see no significant dependence of sampled peptide conformations on their corresponding vdW contributions.

In Figure 2c, the trend in the electrostatic component gives the overall shape of the free energy of solvation trends and differs significantly from the vdW component which is more constant with respect to conformation yet gives the overall ordering of the relative free energies. We find water is the most electrostatically favorable solution and the ternary solution is the least favorable. The magnitudes of the electrostatic values are much larger in magnitude compared with those of the vdW components. The TMAO rescue phenomenon of urea is also not from the electrostatic component of the solvation free energy, as the ternary solution is even more electrostatically unfavorable than the binary TMAO solution. The electrostatic contributions for each of the peptide conformations in the binary TMAO and urea solutions are similar, though the urea values are always smaller than that in TMAO solution. On the other hand, Figure 2a shows that the total solvation free energy for urea is significantly less than that of TMAO. Therefore, in the case of the binary solutions, it is the difference between the behaviors of the vdW contribution in the osmolyte solutions that is mainly responsible for differentiating between the overall solution environments for the peptide conformations.

Transfer free energy changes were calculated for all conformations by subtracting the solvation free energy of water for the conformation from the solvation free energy of the conformation in each of the osmolyte solutions.[27,37] The components to the transfer free energy change were also calculated in this manner. Figure 3a is the total transfer free energy for all conformations into the three osmolyte solutions. In binary TMAO solution, the helix conformation is the most stable vs water as compared to the denatured conformations. In binary urea solution, the trend is the opposite, with the helix conformation being among the most unfavorable and the fully extended being the most favorable. By choosing several representative conformations, from extended to helix, our data is consistent with the idea that TMAO destabilizes the unfolded state, whereas urea stabilizes the denatured state.[38,39] Clearly, we do not have a complete denatured ensemble and there can be dangers in attributing such characteristics to a small number of representatives of larger ensembles. The compensatory effect of TMAO is demonstrated in the total transfer free energy changes, as the values in the ternary solution for each peptide conformation are greater than the binary urea solution, approaching that of the pure water values. In contrast to the binary urea solution, the helix conformation is now the most favorable conformation upon the addition of TMAO. Therefore,

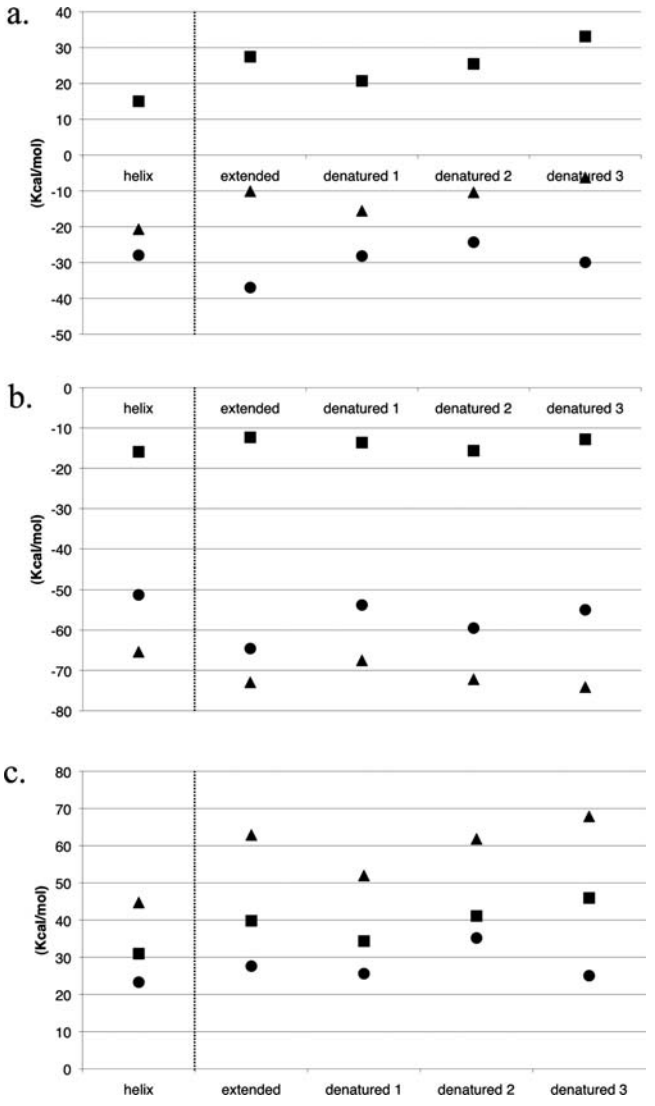

Figure 3. Transfer free energy of five fixed peptide conformations from pure water to TMAO solution (squares), to urea solution (circles), and to TMAO/urea solution (triangles). (a) Total transfer free energy, (b) vdW component of the transfer free energy, and (c) electrostatic component of the transfer free energy.

the trends in the transfer free energies become similar to that of the binary TMAO solution.

Figure 3b clearly indicates the strongly favorable vdW component to the transfer free energy of the urea solution with respect to water. This is in contrast to the TMAO solution, which has a much smaller vdW contribution. Even if taking into account that the urea molarity is double that of TMAO molarity and that urea consists of 8 atoms whereas TMAO consists of 14 atoms, it is clear that the urea vdW component is more favorable than TMAO. The ternary solution has the most favorable vdW component, and is roughly the sum of the contribution from the binary TMAO and urea solutions. Because the vdW component represents short-range interactions, it indicates that TMAO and urea in ternary solution do not compete with each other to make contact with the peptide, even though the osmolyte concentration in the ternary solution is very high.

Figure 3c shows that the electrostatic component of the transfer free energy is very unfavorable compared to water for all osmolyte solutions, with the binary TMAO solution being slightly more unfavorable than urea solution. The ternary solution is the most unfavorable, although the electrostatic component to the transfer free energy to the ternary solution is less than the sum of the binary TMAO and urea solutions. Therefore, as seen with the solvation free energies, the transfer of the peptide conformations to binary urea solution is dominated by the favorable vdW contribution, which overcomes the unfavorable electrostatic contribution and creates a better solution environment for the peptide. This is in contrast with the binary TMAO solution that does not have a significant favorable contribution from the vdW component to balance the strongly unfavorable electrostatic component and causes the TMAO solution to be an unfavorable solution environment for the peptide.

The balance between the transfer free energy components for the ternary osmolyte solution is comparable to that seen in the TMAO solution, albeit at differing magnitudes. Even though the vdW component for the mixture solution is more favorable than the binary urea solution, the electrostatic component is significantly more unfavorable than the binary solution. Therefore, as seen in the binary TMAO solution, the increase in the unfavorability of the electrostatic component of the ternary solution balances the favorable vdW contribution. This produces, in the ternary solution, an environment similar to that of pure water. The electrostatic component of the transfer free energy for the ternary and binary TMAO solution demonstrates the same conformational profile as that of the total transfer free energies, whereas the binary urea solutions does not display such a trend.

Standard fixed-peptide simulations of the solution behavior of all the systems allow further interpretation of the thermodynamic data presented above. We performed 20 ns simulations at NPT condition for these 20 systems maintaining fixed peptide conformations. Table 3 presents a geometric-hydrogen bond analysis of the components between the solution and peptide. Comparing the two binary osmolyte solutions, we see that the urea solution has slightly more total hydrogen bonds between the solution and the peptide conformations as compared to all other solutions. TMAO rarely forms hydrogen bonds with the peptide conformations, which is demonstrated by the relatively small average value and also by the increase in water hydrogen bonds with the peptide as compared to the urea solution. This is expected from the Timasheff idea of preferential exclusion for cosolvents that stabilize folded conformations.

It is interesting that the total number of hydrogen bonds between the peptide and solvent in pure water and in urea solution is almost the same. However, the component analysis shows that the decrease of peptide−water hydrogen bonds is almost completely compensated by the increase of peptide−urea hydrogen bond in urea solution, with urea replacing water for hydrogen bonds with the peptide. This again indicates a direct interaction between peptide and urea. The importance of the direct interaction of urea with proteins for urea destabilization has been well-documented.[11,40−44] The total number of peptide−solvent hydrogen bonds in the ternary solution is comparatively similar to that of the TMAO solution, which is less than that of the binary urea solution. Interestingly, the addition of a second osmolyte does not seem to disturb the interactions between the individual osmolyte and the peptide conformations, since the average number of osmolyte peptide hydrogen bonds with the peptides is similar to that of the binary solution. The largest differences arise from the decrease in the number of water hydrogen bonds with the peptide conformations as compared to the other solutions.

Table 3. Average Number of Hydrogen Bonds and Their Components between Decaalanine Peptide and Solvent Molecules Calculated from 20 ns MD Simulations[a]

in water			Ala−water
helix			15.35
denatured 1			22.77
denatured 2			26.74
denatured 3			29.46
extended			28.36
in 4 M TMAO	**Ala-−TMAO**	**Ala−water**	**total**
helix	0.15	11.40	11.55
denatured 1	0.70	18.12	18.82
denatured 2	0.56	20.95	21.50
denatured 3	0.87	23.37	24.24
extended	1.14	22.36	23.50
in 8 M urea	**Ala−urea**	**Ala−water**	**total**
helix	5.18	9.99	15.17
denatured 1	10.58	13.39	23.97
denatured 2	10.86	17.52	28.37
denatured 3	11.78	19.41	31.20
extended	10.65	19.21	29.87

in TMAO/urea	Ala−TMAO	Ala−urea	Ala−water	total
helix	0.20	4.90	6.40	11.51
denatured 1	0.30	10.51	9.21	20.02
denatured 2	0.52	9.85	13.42	23.79
denatured 3	1.10	12.74	12.73	26.57
extended	1.17	11.35	12.36	24.88

[a] A hydrogen bond here is defined when the distance between heavy atoms (D and O: D−H···O) is between 2.5 and 3.5 Å and the angle 180° D−H···O is less than 60°.

Table 4. Average Number of Hydrogen Bonds and Their Components between Solvent Molecules Calculated from 6 ns Solvent-Only Simulations[a]

TMAO hydrogen bonds	TMAO−urea	TMAO−water	total
in 4 M TMAO	−	2.33	2.33
in TMAO/urea	0.64	1.62	2.26
urea hydrogen bonds	**urea−TMAO**	**urea−urea**	**urea−water**	**total**
in 8 M urea	−	0.54	4.00	4.53
in TMAO/urea	0.32	0.61	2.78	3.71
water hydrogen bonds	**water−TMAO**	**water−urea**	**water−water**	**total**
in pure water	−	−	2.12	2.12
in 4 M TMAO	0.23	−	1.75	1.98
in 8 M urea	−	0.90	1.66	2.56
in TMAO/urea	0.30	1.02	1.15	2.47

[a] A hydrogen bond here is defined when the distance between heavy atoms (D and O: D−H···O) is between 2.5 and 3.5 Å and the angle 180° D−H···O is less than 60°.

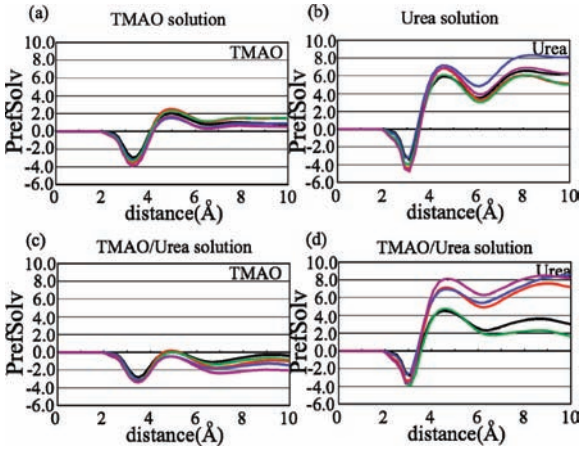

Figure 4. Preferential solvation parameters around the five fixed peptide conformations. (a) TMAO in TMAO solution. (b) Urea in urea solution. (c) TMAO in TMAO/urea solution. (d) Urea in TMAO/urea solution. Black: helix, blue: denatured 1, green: denatured 2, purple: denatured 3, and red: extended. A 20 ns simulation was used.

In Table 4 hydrogen bonding among the solution components can also be analyzed from 6 ns long pure solvent simulations, which allows for the analysis of solvent properties without the influence of the peptide. There is no indication of an increase in the water hydrogen bonding structure caused by the addition of TMAO, nor any indication of a decrease in the water structure caused by urea by this measure.

It is also interesting to note that the total number of solution hydrogen bonds per TMAO molecule is similar in the ternary solution, even though TMAO−water hydrogen bonds are decreased. This is because TMAO is being slightly solvated by urea. In contrast, the total number of hydrogen bonds per urea molecule is decreased in the ternary osmolyte solutions. Therefore, the addition of TMAO to urea solution appears to disrupt the hydrogen bonding network of urea. Most notably, the urea−water hydrogen bonds are decreased, with the hydrogen bonding between urea and TMAO not able to compensate for this decrease. This lack of hydrogen bonding of urea with water can be viewed in terms of the strong hydration properties of TMAO as shown in Figure 4 below.[21,45−51] Recently, data obtained from neutron scattering measurements, and refined using parameters used in previous molecular dynamics simulations,[15,52] suggested that a complex between TMAO and urea is formed by hydrogen bonding.[53] Though our hydrogen bond analysis for the binary solution corresponds well with the previous results, approximately two to three hydrogen bonds between water and TMAO, we do not see any significant hydrogen bond formation between urea and TMAO. Rather, we see less than one hydrogen bond formed between the two osmolytes.

The difference between the local osmolyte environment surrounding the peptide conformations and that of the ideal solution is described by the preferential solvation parameter in Figure 4. This cumulative difference in solvation numbers is difficult to converge numerically, but the trends are certainly visible. The higher values of the preferential solvation parameter between the peptide and urea in the binary solution indicate preferential enhancement of urea around all of the peptide conformations. In contrast, the preferential solvation parameter of TMAO and the peptides in the binary osmolyte solution is much smaller than that of urea and close to zero. This again demonstrates that urea prefers to interact more with the peptide than does TMAO. These results correspond well with the classical dialysis experiments of Timasheff,[39,54] as well as previous predictions.[21,27,55]

dx.doi.org/10.1021/ja1078128 |J. Am. Chem. Soc. 2011, 133, 1849–1858

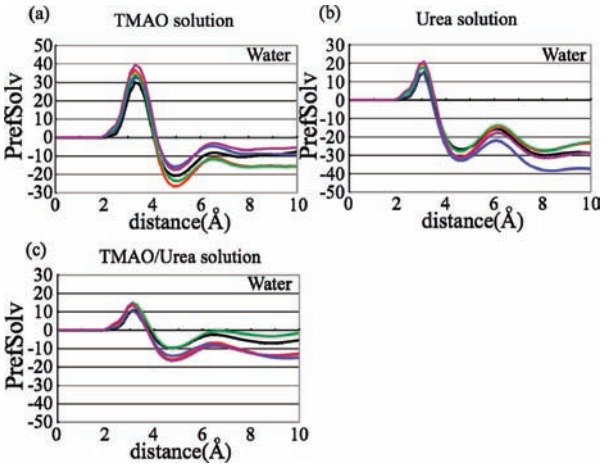

Figure 5. Preferential solvation parameters around the five fixed peptide conformations. (a) Water in TMAO solution. (b) Water in urea solution. (c) Water in TMAO/urea solution. Black: helix, blue: denatured 1, green: denatured 2, purple: denatured 3, and red: extended. A 20 ns simulation was used.

Comparing the preferential solvation parameter of each osmolyte in the respective binary solutions with the ternary solution allows a description of any changes in local distribution of each osmolyte. The preferential solvation parameter between the peptide conformations and urea in the ternary solution displays the same range of values as that of the binary solution. Even with the addition of TMAO to a urea solution, the urea excess around the peptide is not perturbed by TMAO and there still exists an excess of urea molecules in the local region of the peptide conformations. Though individual conformations differ in their values between the binary and ternary solutions, the general tendency of the parameter is significant. Our results show that TMAO does not rescue urea denaturation by removing urea molecules surrounding peptide. The preferential solvation parameter of TMAO in the ternary solution demonstrates the preferential exclusion of TMAO from the local region of all of the peptide conformations as compared to urea. Therefore, the preferential solvation analysis suggests that in a mixture solution of TMAO and urea, the presence of TMAO does little to perturb the preferential interaction of urea with the peptides.

The preferential solvation parameter for water around the peptide is shown in Figure 5. The first peak of the parameter corresponds to the first hydration layer of the peptide (direct interaction of water). The peak is the largest in TMAO as the exclusion of TMAO creates a better first hydration layer for the peptide.[21] We see the largest deficit of water around the peptide in urea solution in Figure 5b, which corresponds to the strong preferential interaction of urea with the peptide in Figure 4b. We also see the deficit of water in the mixture solution in Figure 5b mostly due to the strong excess of urea.

Figure 6 shows the preferential solvation parameters for solvent molecules calculated from the solvent only simulations. Figure 6c shows the water preferential solvation parameter around TMAO, urea, or water species. The most noticeable observation is the strong water preferential solvation parameter around TMAO in the TMAO binary solution. Figure 6a shows the extent TMAO preferential solvation around TMAO, urea, or water species. We see TMAO excess

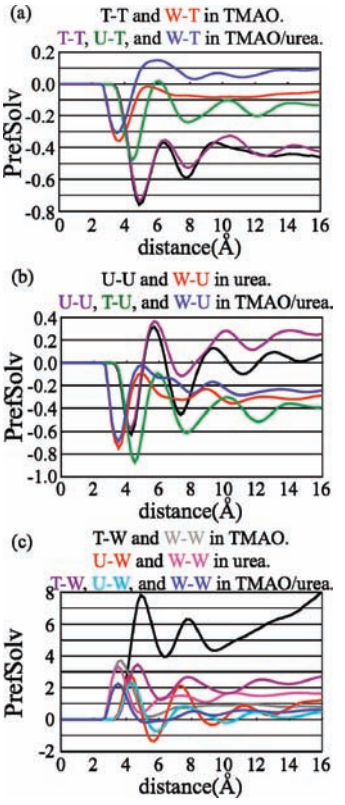

Figure 6. Preferential solvation parameters among solvent molecules analyzed from solvent simulations without peptide. (a) TMAO preferential solvation around TMAO, urea, or water. (b) Urea preferential solvation around TMAO, urea, or water. (c) Water preferential solvation around TMAO, urea, or water. T, U, and W are the abbreviations of TMAO, urea, and water, and A−B means the preferential solvation of B around A. Six nanosecond simulation was used.

only around water molecules, and no indication for complex formation between TMAO and urea. The strong TMAO deficit around TMAO is observed for both TMAO binary solution and the ternary solution especially due to the strong exclusion from the first solvation shell of TMAO. Figure 6b shows urea preferential solvation around TMAO, urea, or water. Again we see no evidence for a near stoichiometric complex formation between urea and TMAO.

Figure 7 shows regions of high solvent density around the peptide in the case of the extended peptide conformation, with green, purple, and red corresponding to TMAO, urea, and water, respectively. We see that TMAO is found in regions similar to that in which urea accumulates not only in the binary TMAO or urea solution but also in TMAO/urea mixture solution. Also, it is evident that all solution components tend to maintain their region of accumulation even considering the competition for the same sites. This indicates that the solvent profiles around the peptide are not perturbed by the addition of another osmolyte species. In other words, urea excess around the peptide was not disturbed by the addition of TMAO. This is consistent with the observed urea excess around the peptide that was similar in both TMAO/urea solution as in urea solution in Figure 4. It is also consistent with that the vdW component of the transfer solvation free energy in the ternary TMAO/urea solution that was approximately equal to the sum of the binary TMAO and urea solutions as seen in Figure 3b.

dx.doi.org/10.1021/ja1078128 |J. Am. Chem. Soc. 2011, 133, 1849–1858

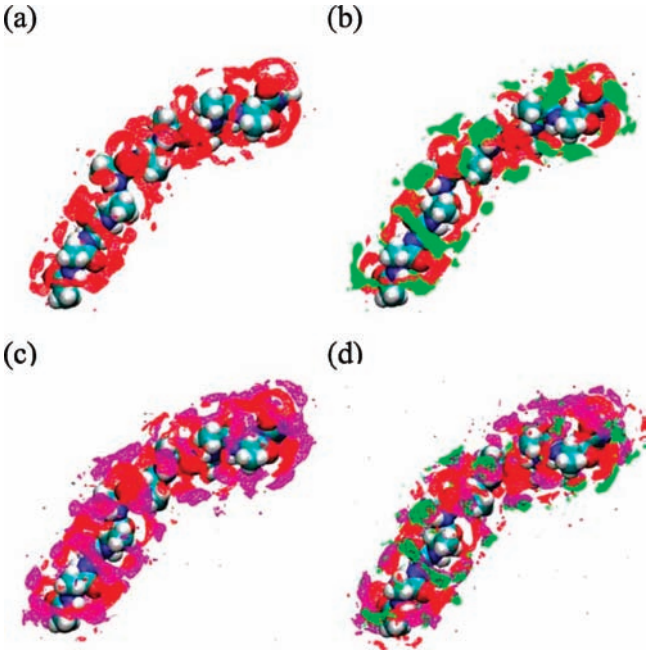

Figure 7. Density map around the extended conformation (a) in pure water, (b) in TMAO solution, (c) in urea solution, and (d) in TMAO/urea solution. Green, purple, and red are TMAO, urea, and water density, respectively. We first picked up 6000 snapshots at even interval from 6.0 ns fixed peptide simulations, and then the center of mass of solvent molecules is calculated for each snapshot. The volume is divided into a grid by using 0.5 $Å^3$ boxes. The regions with density more than several times uniform density are shown. We chose 6 times (TMAO), 4 times (urea), and 2.5 times (water) as the threshold values over bulk density in order to make easily viewable figures. These threshold values were used for all four solutions.

4. CONCLUSIONS

We have calculated the solvation and transfer free energies of a decaalanine peptide in folded and varying states of denaturation in several osmolyte solutions. One of the benefits of computationally calculated solvation free energies is the ability to distinguish the solvation free energies of different states in the folded and denatured ensemble. We also decomposed the contribution of the electrostatic and vdW interactions to the total free energy, thus allowing a more detailed analysis of the mechanism of (de)stabilization. We abandon the classical separation of electrostatic and hydrophobic effects. We find the more natural set of variables, electrostatic and vdW contributions, to better show the mechanistic trends of solution (de)stabilization without the problems of relevance[16] and multiply definitions[36] such as hydrophobicity.

Our results here strongly suggest the importance of the vdW contribution to the solvation effect of urea as seen previously.[11,27] It is the favorable vdW contribution, caused by the excess of urea molecules around the peptide that allows for the overall urea solution to become more free energetically favorable as compared to pure water. This vdW contribution in the binary urea solution overcomes the unfavorable electrostatic contributions, as compared to pure water. Also, relative to water, urea has more favorable vdW interactions with the denatured states, thus allowing urea to stabilize the extended states more than the compact helix as shown in Figure 3b.

On the other hand, in the binary TMAO solution the vdW contribution is smaller than urea, though more favorable than water. Because the favorability of the vdW component cannot overcome the unfavorability of the electrostatic loss, this solution is higher in free energy for all peptide conformations, thus decreasing peptide solubility.[27] This effect becomes more significant as the exposed area of the peptide becomes larger. Therefore, the compact helix state becomes more stable than the denatured states in the binary TMAO solution. In this sense, our data indicates that TMAO solutions prefers compact states, thus stabilizing the native state.[21]

This trend in the trade-off between the vdW and electrostatic contributions may be viewed in a similar manner in the ternary solution. The osmolyte mixture solution possesses the most favorable vdW contribution (appearing to be roughly similar to the cumulative total between TMAO and urea binary solutions); however the electrostatic component is significantly more unfavorable. Therefore, as seen in the binary TMAO solution, the favorability of the vdW free energy contribution is not enough to counter the strongly unfavorable electrostatic contribution. However, in the ternary solution the vdW and electrostatic component are of roughly equivalent magnitude, thus producing a solution environment that approaches that of water in terms of the relative free energy.

Several models for TMAO compensation of urea destabilization have been proposed. Previous simulations have suggested an increase in the water hydrogen bond network caused by the addition of TMAO and thus attribute the TMAO compensatory effect to the inability of water to hydrate the unfolded conformations.[52] However, others were not able to recreate the substantial increase in the strength of the water hydrogen bonds upon the addition of TMAO to urea solution.[15] Similarly, no evidence of an increase of the water hydrogen bond structure in simulations of a peptide backbone model in aqueous TMAO solution was seen.[21] The data presented here also demonstrates no evidence for an increase in the water structure in binary aqueous TMAO solution or in the mixture osmolyte solution. Clearly, model differences are partially responsible for the variety of mechanistic interpretations, and our choice of model impacts the current study.

A separate physical model was proposed based upon simulation studies of osmolyte solutions and osmolytes with hydrophobic solutes.[14,15] The authors noted the strong interaction potentials of water and urea with TMAO and suggest a preferential solvation mechanism for TMAO-counteraction, whereby urea and water prefer to solvate TMAO as compared to the peptide.[15] Though this model makes intuitive sense, as TMAO is known for its strong hydrogen bonding propensity, due to the dative bond,[50] the system studied lacked peptide. In separate simulations, the authors demonstrated the complete disruption of neopentane self-interaction (contact correlations), thus making it unlikely that TMAO counteracts urea denaturation by increasing hydrophobic interactions[14] in agreement with experiment.[16]

Corresponding to the preferential solvation mechanism, our results presented here indicate a decrease in the number of water hydrogen bonds with the peptide in TMAO. However, this is not marked by a concurrent decrease in the number of urea hydrogen bonds with the peptide backbone, a necessary component of the mechanism. Similarly, we do not see an increase in the number of TMAO and water hydrogen bonds. Cumulatively, TMAO forms the same number of hydrogen bonds per molecule, as urea is able to slightly solvate TMAO. The same is not the case for urea, as TMAO does not appreciably solvate urea for our model, thus leading to an overall decrease in the number of hydrogen bonds

per urea molecule. Implicit to the classic preferential solvation rescue mechanism is a disruption in the nature by which urea interacts with the peptide. However, based on our hydrogen bond and preferential interaction analysis, we see no evidence for a disruption in the nature of molecular interaction between urea and the peptide. Similarly, experimental studies strongly suggest that the presence of a competing osmolyte does not interfere with the efficiency of the other osmolyte to act on the peptide.[12,13] A recent study[53] that utilized the same simulation parameters as previously mentioned,[15] suggested stoichiometric complex formation via hydrogen bonding between TMAO and urea. However, the results presented here show no indication of significant correlations, let alone stoichiometric complexes, between TMAO and urea molecules.

Our results demonstrate a clear lack of disruption of the correlations responsible for the manner in which the two osmolyte species interact with the peptide: urea remains in excess locally, whereas TMAO remains excluded. The free energy changes are explainable by comparing and contrasting the well-defined electrostatic and vdW contributions (as opposed to electrostatic and the more broadly, often phenomenologically defined concept of hydrophobicity). Thus, the accumulation of urea responsible for the favorable free energy of the oligo alanine models in urea solution is dominated by the favorable vdW component for the change in free energy from water to urea of the peptide models. Correspondingly, the lack of interaction of the protecting osmolyte TMAO with the alanine oligomers does not result in favorable vdW interactions and instead contributes to the overall unfavorable solvation difference of the models for TMAO versus water. The results here demonstrate the utility of concepts using molecular interaction components to understand the osmolyte effect on protein stability. We feel molecular interaction components provide clarity often lacking when discussing effects in terms of phenomenological or multiply defined concepts like hydrophobicity.

Caution must be used extrapolating the results from this simple system to full proteins. We have examined the specific system of decaalanine, and we cannot directly expand all our observations to all protein systems although we chose to demonstrate the concepts presented using this alanine model system because the α helix is an important structural component of proteins.

AUTHOR INFORMATION

Corresponding Author
pettitt@uh.edu

ACKNOWLEDGMENT

We are grateful for the insight, discussions, and collegiality provided by Wayne Bolen, Jörg Rösgen, and Matthew Auton. We also acknowledge partial financial support from the National Institutes of Health (GM037657 and GM049760) and the R. A. Welch foundation (E-1028). Partial financial support for CYH at the beginning of this project was provided by NIH Molecular Biophysics Training Grant (Houston Area Molecular Biophysics Program T32 GM008280). The simulations and computations were performed using the Molecular Science Computing Facility at the Environmental Research of the U.S. Department of Energy, located at the Pacific Northwest National Laboratory, and the Pittsburgh Supercomputing Center on the National Science Foundation Teragrid.

REFERENCES

(1) Hochachka, P. W., Somero, G. N. *Biochemical Adaptation. Mechanism and process in physiological evolution*; Oxford University Press: New York, 2002.
(2) Yancey, P.; Clark, M.; Hand, S.; Bowlus, R.; Somero, G. *Science* **1982**, *217*, 1214.
(3) Yancey, P. H. *J. Exp. Biol.* **2005**, *208*, 2819.
(4) Lin, T. Y.; Timasheff, S. N. *Biochemistry* **1994**, *33*, 12695.
(5) Wang, A.; Bolen, D. *Biochemistry* **1997**, *36*, 9101.
(6) Yancey, P. H.; Somero, G. N. *Biochem. J.* **1979**, *183*, 317.
(7) Baskakov, I.; Wang, A.; Bolen, D. W. *Biophys. J.* **1998**, *74*, 2666.
(8) Bolen, D. W.; Rose, G. D. *Annu. Rev. Biochem.* **2008**, *77*, 339.
(9) Rose, G.; Fleming, P.; Banavar, J.; Maritan, A. *Proc. Natl. Acad. Sci. U.S.A.* **2006**, *103*, 16623.
(10) Auton, M.; Bolen, D. *Proc. Natl. Acad. Sci. U.S.A.* **2005**, *102*, 15065.
(11) Hua, L.; Zhou, R.; Thirumalai, D.; Berne, B. J. *Proc. Natl. Acad. Sci. U.S.A.* **2008**, *105*, 16928.
(12) Mello, C.; Barrick, D. *Protein Sci.* **2003**, *12*, 1522.
(13) Holthauzen, L. M.; Bolen, D. W. *Protein Sci.* **2007**, *16*, 293.
(14) Paul, S.; Patey, G. N. *J. Phys. Chem. B* **2007**, *111*, 7932.
(15) Paul, S.; Patey, G. *J. Am. Chem. Soc.* **2007**, *129*, 4476.
(16) Auton, M.; Holthauzen, L.; Bolen, D. *Proc. Natl. Acad. Sci. U.S. A.* **2007**, *104*, 15317.
(17) Duan, Y.; Wu, C.; Chowdhury, S.; Lee, M. C.; Xiong, G.; Zhang, W.; Yang, R.; Cieplak, P.; Luo, R.; Lee, T.; Caldwell, J.; Wang, J.; Kollman, P. *J. Comput. Chem.* **2003**, *24*, 1999.
(18) Kast, K. M.; Brickmann, J.; Kast, S. M.; Berry, R. S. *J. Phys. Chem. A* **2003**, *107*, 5342.
(19) Weerasinghe, S.; Smith, P. E. *J. Phys. Chem. B* **2003**, *107*, 3891.
(20) Jorgensen, W. L.; Chandrasekhar, J.; Madura, J. D.; Impey, R. W.; Klein, M. L. *J. Chem. Phys.* **1983**, *79*, 926.
(21) Hu, C. Y.; Lynch, G. C.; Kokubo, H.; Pettitt, B. M. *Proteins* **2010**, *78*, 695.
(22) Kokubo, H.; Pettitt, B. *J. Phys. Chem. B* **2007**, *111*, 5233.
(23) Nose, S. *J. Chem. Phys.* **1984**, *81*, 511.
(24) Andersen, H. C. *J. Chem. Phys.* **1980**, *72*, 2384.
(25) Andersen, H. C. *J. Comput. Phys.* **1983**, *52*, 24.
(26) Ewald, P. *Ann. Phys.* **1921**, *64*, 253.
(27) Hu, C. Y.; Kokubo, H.; Lynch, G. C.; Bolen, D. W.; Pettitt, B. M. *Protein Sci.* **2010**, *19*, 1011.
(28) Jiang, W.; Hodoscek, M.; Roux, B. *J. Chem. Theory Comput.* **2009**, *5*, 2583.
(29) Gunsteren, W. F. v. In *Computer Simulation of Biomolecular Systems*; Weiner, W. F. v. G. a. P. K., Ed.; Escom: Leiden, 1989, p 27.
(30) Fukunishi, H.; Watanabe, O.; Takada, S. *J. Chem. Phys.* **2002**, *116*, 9058.
(31) Sugita, Y.; Kitao, A.; Okamoto, Y. *J. Chem. Phys.* **2000**, *113*, 6042.
(32) Beutler, T. C.; Mark, A. E.; Vanschaik, R. C.; Gerber, P. R.; van Gunsteren, W. F. *Chem. Phys. Lett.* **1994**, *222*, 529.
(33) Zacharias, M.; Straatsma, T. P.; McCammon, J. A. *J. Chem. Phys.* **1994**, *100*, 9025.
(34) Shirts, M.; Pande, V. *J. Chem. Phys.* **2005**, *122*, 144107.
(35) Shirts, M.; Pitera, J.; Swope, W.; Pande, V. *J. Chem. Phys.* **2003**, *119*, 5740.
(36) Chandler, D. *Nature* **2005**, *437*, 640.
(37) Staritzbichler, R.; Gu, W.; Helms, V. *J. Phys. Chem. B* **2005**, *109*, 19000.
(38) Arakawa, T.; Bhat, R.; Timasheff, S. N. *Biochemistry* **1990**, *29*, 1924.
(39) Lee, J. C.; Timaseff, S. N. *J. Biol. Chem.* **1981**, *256*, 7193.
(40) Das, A.; Mukhopadhyay, C. *J. Phys. Chem. B* **2009**, *113*, 12816.
(41) Lim, W. K.; Rösgen, J.; Englander, S. W. *Proc. Natl. Acad. Sci. U.S.A.* **2009**, *106*, 2595.
(42) Robinson, D. R.; Jencks, W. P. *J. Am. Chem. Soc.* **1965**, *87*, 2462.
(43) Caflisch, A.; Karplus, M. *Structure* **1999**, *7*, 477.

(44) Stumpe, M. C.; Grubmüller, H. *J. Am. Chem. Soc.* **2007**, *129*, 16126.
(45) Di Michele, A.; Freda, M.; Onori, G.; Paolantoni, M.; Santucci, A.; Sassi, P. *J. Phys. Chem. B* **2006**, *110*, 21077.
(46) Fornili, A.; Civera, M.; Sironi, M.; Fornili, S. *Phys. Chem. Chem. Phys.* **2003**, *5*, 4905.
(47) Freda, M.; Onori, G.; Santucci, A. *J. Phys. Chem. B* **2001**, *105*, 12714.
(48) Freda, M.; Onori, G.; Santucci, A. *Phys. Chem. Chem. Phys.* **2002**, *4*, 4979.
(49) Michele, A.; Freda, M.; Onori, G.; Santucci, A. *J. Phys. Chem. A* **2004**, *108*, 6145.
(50) Paul, S.; Patey, G. *J. Phys. Chem. B* **2006**, *110*, 10514.
(51) Sinibaldi, R.; Casieri, C.; Melchionna, S.; Onori, G.; Segre, A. L.; Viel, S.; Mannina, L.; De Luca, F. *J. Phys. Chem. B* **2006**, *110*, 8885.
(52) Zou, Q.; Bennion, B.; Daggett, V.; Murphy, K. *J. Am. Chem. Soc.* **2002**, *124*, 1192.
(53) Meersman, F.; Bowron, D.; Soper, A. K.; Koch, M. H. J. *Biophys. J.* **2009**, *97*, 2559.
(54) Timasheff, S. *Biochemistry* **1992**, *31*, 9857.
(55) Auton, M.; Bolen, D. W.; Rösgen, J. *Proteins* **2008**, *73*, 802.